Available online at www.sciencedirect.com
ScienceDirect
Surface & Coatings Technology 202 (2008) 3571–3578
SURFACE & COATINGS TECHNOLOGY
www.elsevier.com/locate/surfcoat

Electroless copper deposition on a pitch-based activated carbon fiber and an application for NO removal

Jeong Hoon Byeon [a], Hee Seung Yoon [b], Ki Young Yoon [a], Seung Kon Ryu [b], Jungho Hwang [a,*]

[a] School of Mechanical Engineering, Yonsei University, Seoul 120-749, Republic of Korea
[b] School of Chemical Engineering, Chungnam National University, Daejeon 305-764, Republic of Korea

Received 31 October 2007; accepted in revised form 21 December 2007
Available online 28 December 2007

Abstract

Pitch fibers were prepared from petroleum-derived isotropic pitch precursors using melt-blown spinning. Activated carbon fibers (ACF) were formed from pitch fibers and after stabilization, carbonization and steam thermal activation were then further activated with Pd–Sn catalytic nuclei in a single-step process. The activated ACF were then used as supporters in the specific, electroless deposition of fine copper particles. Field emission scanning electron microscopy-energy dispersive X-ray spectroscopy results showed that the ACF were uniformly coated with nearly pure fine copper particles, and the copper content on the ACF increased with deposition time. The amounts of copper on the ACF and their crystalline characteristics were analyzed using an inductively coupled plasma and a X-ray diffractometry, respectively. With the copper particles-deposited on the ACF, the removal of nitrogen monoxide (NO) for four different deposition times (5, 10, 15 and 20 min) was tested. Experiments on the removal of NO were carried out in a packed bed tubular reactor with various reaction temperatures ranging between 423 and 673 K. For all deposition times, the NO removal efficiency increased with increasing reaction temperature up to 673 K. The NO removal efficiency was the highest when the amount was Cu/ACF = 110 mg/g (deposition time of 5 min), however, decreased at Cu/ACF beyond 110 mg/g (deposition times of 10, 15, 20 min) due to the decreased adsorption as a result of the increased amount of copper.

PACS: 61.30.Hn; 61.46.Df; 68.47.De; 71.20.Be; 78.55.Mb; 81.05.Ni; 81.16.Hc; 82.47.Wx; 92.60.Sz
Keywords: Activated carbon fibers; Single-step activation; Electroless deposition; NO removal; Adsorption property

1. Introduction

Porous carbon materials, due to their extensive specific surface area, high adsorption capacity, microstructure, and special surface reactivity, have been widely used in separation, purification, and catalytic processes [1]. Activated carbon fibers (ACF), highly microporous carbon materials [2–4], are commercially available in the form of fiber tows, cloths (fabrics), papers, mats and felts [5]. ACF have a larger micropore volume and a more uniform micropore size distribution than granular activated carbons (GAC) and; thus, are considered to have a larger adsorption capacity and greater adsorption and desorption rates [6–11].

The ACF may be packed or constructed to fit almost any geometry for almost any catalytic application and satisfies the requirements of high catalyst effectiveness and a low pressure drop for finely divided catalysts, but avoids the technical problems associated with powders. For example, the ACF may be employed for the removal of NO_x [12–16], but only physically adsorbs a limited amount of NO because of the weak interactions between the two [17,18]. The catalytic reduction of NO to N_2 and O_2 using ACF employing a transition metal (Ni, Fe, Cu, or Pd) prepared by the impregnation and precipitation of an aqueous solution of the metal, has previously been investigated [1], copper has been shown to possess the most efficient catalytic activity toward the reduction of NO to N_2 and O_2, both with and without O_2 [19,20].

Recently, electrolytic metal deposition, of an aqueous solution of metal ions, has been proposed as a useful method for the

* Corresponding author. Tel.: +82 2 2123 2821; fax: +82 2 312 2821.
E-mail address: hwangjh@yonsei.ac.kr (J. Hwang).

0257-8972/$ - see front matter © 2007 Elsevier B.V. All rights reserved.
doi:10.1016/j.surfcoat.2007.12.032

introduction of a metal onto carbon surfaces and into carbon micropores [1,21]. Electroless metal deposition is a kind of electrolytic metal deposition and can be effective for coating ACF [21–23]. Electroless metal deposition refers to the deposition of a metal onto a substrate, without an external electric current, via oxidation–reduction reactions [24]. The electroless deposition technique enables catalytic components to be easily and uniformly deposited in some channels of supporter with a complex configuration, provided that the deposition solution is in contact with the channel walls [25].

For the stable deposition of fine metal particles onto the ACF, the catalytic activation method proposed by Ang et al. [26] and Xu et al. [27] was employed. These two investigations studied the coating of carbon nanotubes with nickel and copper, respectively. The nanotubes were activated in one activation bath (single-step process). In our study, a single-step process was used to catalytically Pd–Sn activate the ACF and; thus, to introduce metallic Pd sites onto the ACF surfaces for the electroless copper deposition [28]. The metallic Pd sites worked effectively in the electroless deposition of copper due to the galvanic displacement of the metallic Pd by Cu [24,29].

In the present study, pitch-based ACF were first coated with fine particles using electroless copper deposition and then characterized by field emission scanning electron microscopy (FESEM), energy dispersive X-ray spectroscopy (EDX), X-ray diffractometry (XRD), nitrogen adsorption and inductively coupled plasma (ICP) analysis. Finally, the effect of the copper particles on the catalytic reduction of NO was investigated at various reaction temperatures in the absence of oxygen.

2. Experimental

Pitch-based ACF were synthesized using a conventional melt-blown spinning method. The fibers, 1 mm in diameter, were produced, using extruding melt (IPP; SK Chemical Co., Korea) through a round-shaped mono-hole spinneret ($L/D=2$, $D=70$ mm), under pressurized nitrogen at 6 kg/cm^2, 673 K, with subsequent drawing at a take-up speed of 550 m/min. The melt-blown spinning pitch fibers were then oxidatively stabilized in air by heating to 673 K at 1 K/min for 2 h. The stabilized pitch fibers were then carbonized by heating in an N_2 atmosphere to 1273 K at 10 K/min for 30 min. After holding the carbonized fibers at 1223 K for 30 min, they were finally activated in steam (50 vol.%) carried by N_2. These ACF were washed with deionized water and dried overnight at an ambient temperature.

Since the bond strength of the copper particles on the ACF was very sensitive to surface contamination, the ACF were thoroughly degreased by immersing in a diluted degreasing agent bath (50 mL of CC829, Yooil Material Technology, Korea, mixed with 950 mL of DI water) at 327 K for 10 min. After washing the degreased ACF three times with DI water, the palladium and tin species were introduced onto by immersing in a mixed Pd–Sn colloidal solution at 318 K for 6 min. A solution (30 mL of CATA1064, Yooil Material Technology, Korea) diluted with 1 M of nitric acid (970 mL) was used as a mixed Pd–Sn colloidal solution. The catalytically activated ACF were immersed in an acceleration solution bath (50 mL ACCEL95, Yooil Material Technology, Korea, diluted to 1000 mL with DI water) for 7 min at 298 K and then washed with DI water a further three times. The acidic accelerator was used to preferentially dissolve the protective layer (mainly Sn layer), exposing a greater surface area of the catalytic Pd nuclei. When the catalytically activated, accelerated ACF were immersed in an electroless deposition bath, copper was deposited at the catalytic sites, with copper particles-deposited ACF finally obtained. The deposition bath (1 L) consisted of copper sulfate dominant solution (120 mL EC1051A, Yooil Material Technology, Korea, diluted to 500 mL with DI water) and formaldehyde dominant solution (110 mL EC1051B, Yooil Material Technology, Korea, diluted to 500 mL with DI water) at 298 K for various treatment times ranging from 0 to 20 min.

To study the surface structures of the ACF, wide-angle XRD patterns of the ACF were obtained with a Rigaku Model D/MAX-Rint 2000 (Japan) diffraction meter using Cu$K\alpha$ radiation ($\lambda=0.15418$ nm) at 30 kV and 20 mA. A thin powder sample of the ACF was placed onto an oriented monocrystalline quartz plate and scanned from 10° to 80° (2θ) at 4°/min. A FESEM (JSM-6500F, JEOL, Japan) was used to observe the surface morphology of the ACF as well as the distribution of copper particles. A chemical analysis was performed using EDX (JED-2300, JEOL, Japan). The amount of copper particles on the ACF sample was determined using an ICP (Elan 6000, Perkin–Elmer, US). Approximately 0.1 g of the sample was dissolved in

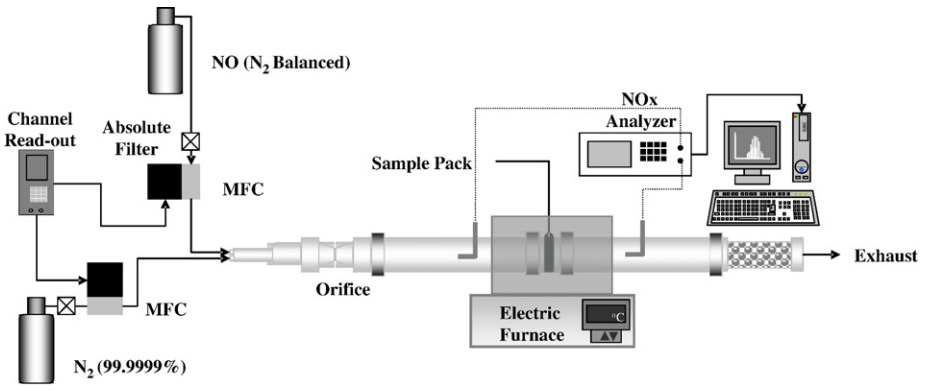

Fig. 1. Diagram of experimental set-up for NO removal test.

50 mL nitric acid, and the mixture was diluted to 100 mL with DI water. After 3 h, the sample was filtered, with the remaining mixture delivered for ICP analysis. The nitrogen adsorption isotherms of an ACF sample were measured using a porosimeter (ASAP 2010, Micromeritics Ins. Corp., US) at 77.4 K with relative pressures ranging from 10^{-6} to 1. High purity (99.9999%) nitrogen was used for a material to be adsorbed. All samples were degassed at 573 K for 2 h before each measurement. The specific surface area was determined using the Brunauer, Emmett, and Teller (BET) equation. The total pore volume, which was estimated on the basis of the N_2 volume adsorbed at a relative saturation pressure (~0.996), actually corresponded to the total amount adsorbed. The pore size distribution was determined using the Barrett, Joyner, and Halenda (BJH) method, which uses the area of the pore walls and the Kelvin equation to correlate the relative N_2 pressure at equilibrium with the amount of porous solid, with the size of the pores where the capillary condensation occurs.

Fig. 1 shows the experimental set-up used for the NO removal test. For each experiment, 3 g of the prepared ACF (140 mm in length) was initially inserted into a quartz tube reactor (10 mm in diameter and 500 mm in length) and heated under an N_2 flow at 423 K for 1 h inside an electric furnace (1 kW). The wall temperature of the reactor increased from 423 to 673 K using a proportional integral derivative (PID) temperature controller. Stainless steel (SS) mesh was used to support the ACF and minimize the channeling phenomenon. Model NO gas in N_2 at room temperature was delivered to the reactor and mixed with N_2 (99.9999%) gas, resulting in a NO concentration of 160 ppm at the reactor inlet. Absolute filters were used

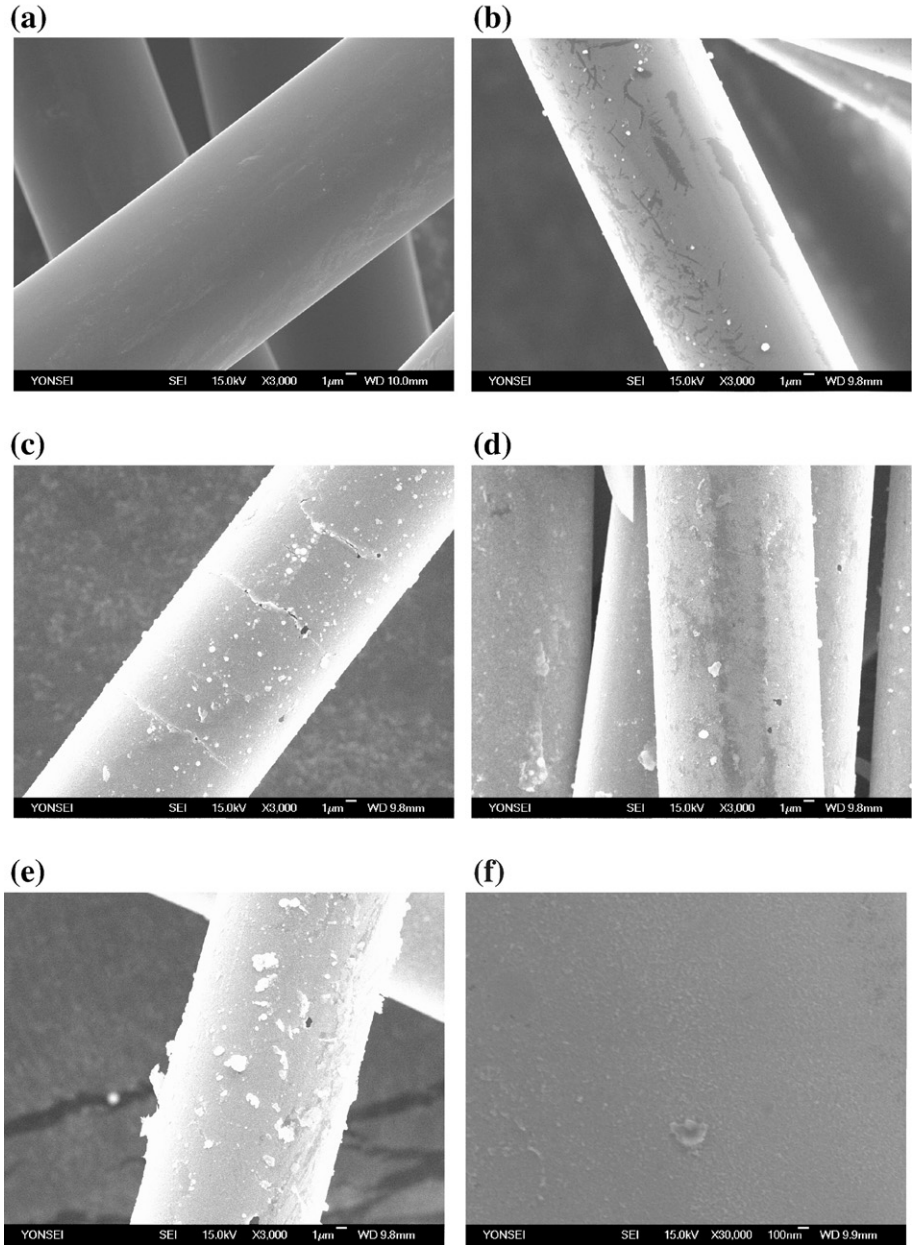

Fig. 2. FESEM micrographs of pristine and copper-deposited ACF. (a) Cu-00 (b) Cu-05 (c) Cu-10 (d) Cu-15 (e) Cu-20 (f) High magnitude micrograph.

to filter out contaminant particulate matters existing in the test gases. The total gas flow rate through the reactor was maintained at 3 L/min by adjusting two mass flow controllers (MKS Instrument, US). An orifice was used to promote mixing of NO and N_2 fluid dynamically.

The concentration of NO was continuously measured using a chemiluminescence NO analyzer (Thermo Electron Instruments Inc., Model 42c, US), which monitors NO at a sampling rate of 0.7 L/min. The NO removal efficiency was determined by measuring the concentration of NO at the outlet of the reactor. Experiments were repeated four times, with the average values reported.

3. Results and discussion

Fig. 2 shows FESEM of ACF samples coated with Cu at different operating time from 5 to 20 min. Cu-05, Cu-10, Cu-15 and Cu-20 represent copper coated ACF for deposition times of 5, 10, 15 and 20 min, respectively, while Cu-00 represents pristine ACF. With increasing deposition time, more particles were deposited onto the surface of a fiber, which grew larger, with "snowflake" shaped particles or aggregates of 50 nm–1 μm observed, as shown in Fig. 2(b) and (e). Additionally, the average sizes of individual copper grains were obtained from SEM micrographs shown in Fig. 2(f). They were 6.8±1.64, 7.4±1.59,

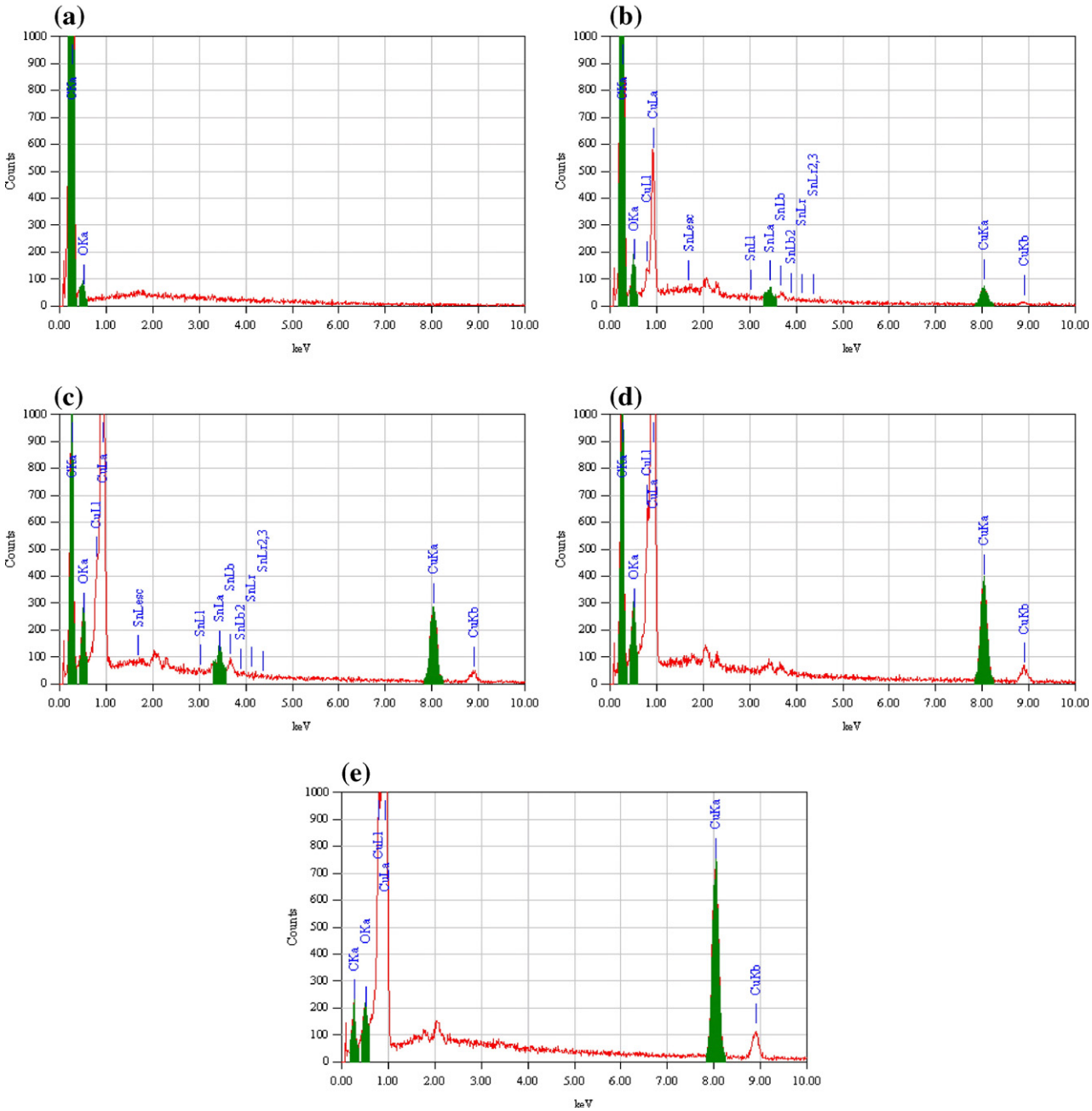

Fig. 3. EDX profiles of pristine and copper-deposited ACF. (a) Cu-00 (b) Cu-05 (c) Cu-10 (d) Cu-15 (e) Cu-20.

14.6±1.58 and 16.8±1.62 nm for Cu-05, Cu-10, Cu-15 and Cu-20, respectively. The SEM micrographs revealed copper particles, as examined by EDX analyses, as shown in Fig. 3. The EDX results showed that an ACF sample contained carbon, copper and a small amount of oxygen. The observed oxygen may have originated from the ACF. Fig. 3 shows that with Cu-00 no copper peak was observed, but the copper-deposited ACF samples had some CuKa and CuLa, etc. peaks, indicating the presence of copper in the ACF samples. The Cu-05 and Cu-10 samples also contained a small amount of tin, which may have originated from the Pd–Sn activation. However, it was interesting that no tin was detected for deposition times longer than 10 min implying the Cu-15 and Cu-20 ACF samples used for the analysis were entirely covered with copper.

The surface structures of the copper particles-deposited ACF samples were also studied using the wide-angle XRD method. Fig. 4 shows sharp peaks at around $2\theta = 43°$, 50° and 74°, which corresponded to the (111), (200) and (220) planes of the copper (JCPDS 4-836) on the ACF surfaces, respectively. The average crystallite sizes estimated from the XRD line broadening of the (111) peak, according to Scherrer's equation ($t = 0.9\lambda/(B\cos\theta)$), were 3.97, 6.85, 12.44 and 14.95 nm for copper deposition times of 5, 10, 15 and 20 min, respectively. The sharpness of the copper peaks proved that the copper particles had a nearly perfect crystal structure. The intensities of the copper peaks increased with deposition time, which was caused by the growth of the copper particles. The intensity of the copper peaks and the crystallinity of the copper-deposited ACF were strengthened with increasing deposition time. From the ICP analyses, the mass of copper per unit mass of ACF was obtained. Fig. 5 shows that the amount of copper increased with increasing deposition time. The specific surface areas of copper were calculated using the data of XRD and ICP, and the results were 19.4, 25.4, 17.0 and 18.3 $m^2 \cdot Cu/g \cdot ACF$ for Cu-05, Cu-10, Cu-15 and Cu-20, respectively.

Once the copper-deposited ACF had been characterized, they were applied as catalyst fibers to enhance the NO removal

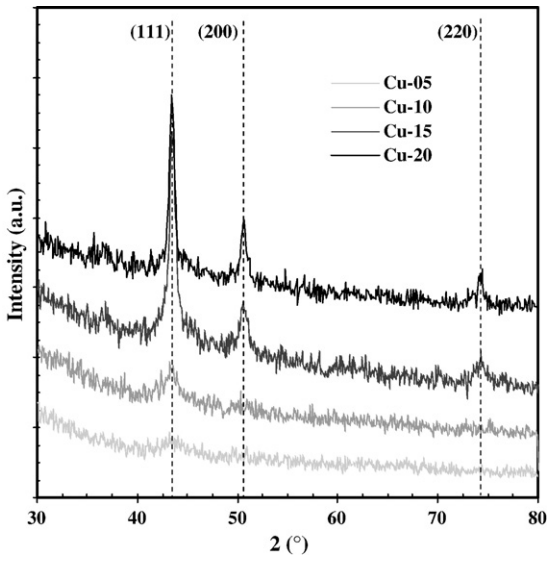

Fig. 4. X-ray diffraction patterns of copper-deposited ACF.

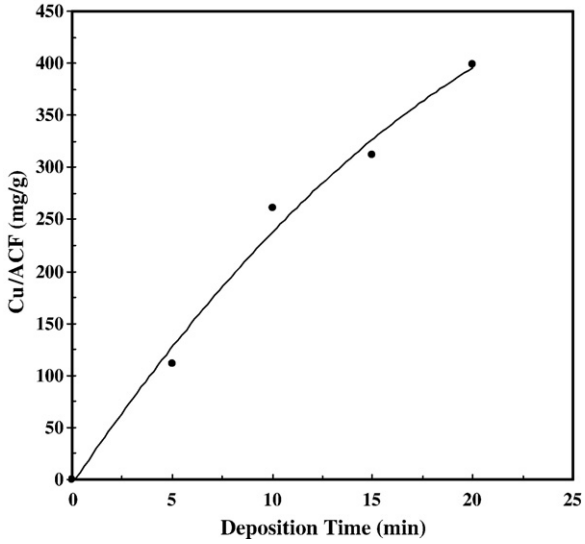

Fig. 5. Amount of copper as a function of deposition time (by ICP analysis).

efficiency. Fig. 6 shows the results under various temperature conditions. The test NO gas was injected into the reactor at a concentration of 160 ppm (N_2 balance). When no copper particles existed on the ACF, NO was adsorbed onto the surface of the carbon fibers, and this adsorption slightly increased with increasing temperature. However, after about 4 min, the adsorption drastically decreased at all temperatures. When copper particles existed on the ACF, in addition to the adsorption by the carbon fibers, NO, which was adsorbed onto the carbon fibers, would transfer to the neighboring copper particles by surface diffusion, resulting in the catalytic reduction of NO around the copper particles. For temperatures below 473 K, the amount of copper on the ACF had little effect on the removal of NO. However, when the temperature was equal to or higher than 573 K, more NO was removed with the copper-deposited samples. At a reaction temperature of 673 K, the removal efficiencies at the steady-state were 80–90%. Of note: for temperatures between 573 and 673 K; however, the highest removal efficiency was achieved with the Cu-05 sample, even though the amount of copper, acting as a catalyst, was lowest. The removal efficiency decreased as the amount of copper was further increased.

To understand the adverse effect of an excessive amount of copper on the removal of NO, the porosity and specific surface area properties of the copper-deposited ACF were measured. Fig. 7 shows that the greatest uptake occurred at a relatively low pressure ($P/P_0 < 0.1$) and reached a plateau at $P/P_0 \approx 0.3$, implying that all the ACF samples, according to the IUPAC classification, had microporous characteristics (type I isotherm) [30]. The specific surface area was largest for the Cu-00, and decreased with increasing amount of copper as the deposited copper particles could block or take up some pores of the corresponding ACF support.

The pore size distributions of the samples were also measured. Fig. 8 shows that the pore size distributions of all the samples were concentrated at pore diameters smaller than 30 Å. Pores within

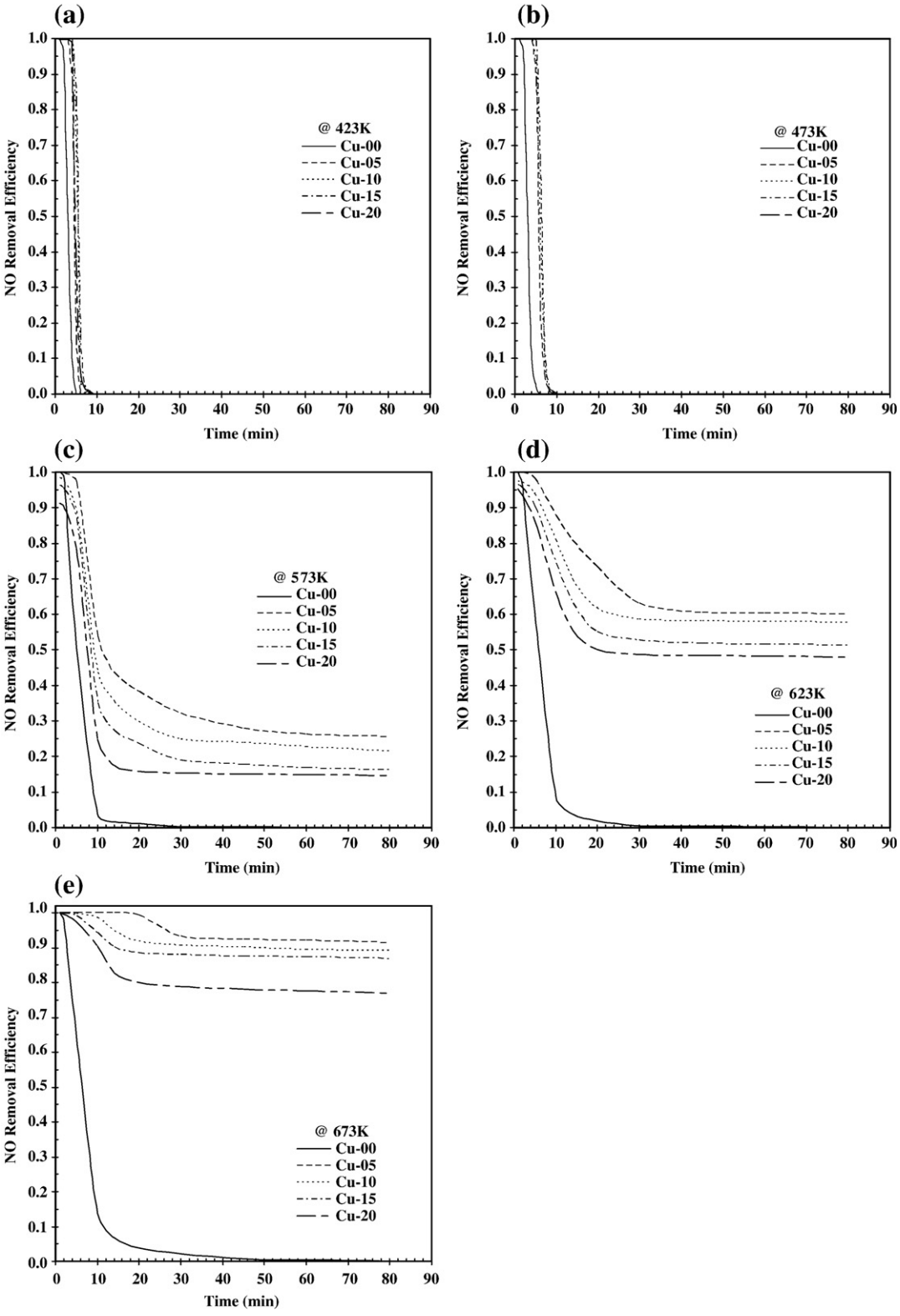

Fig. 6. NO removal characteristics of pristine and copper-deposited ACF. (a) At 423 K (b) At 473 K (c) At 573 K (d) At 623 K (e) At 673 K.

porous materials are typically classified as micropores (<20 Å), mesopores (20–500 Å) and macropores (>500 Å), in accordance with the classification adopted by the IUPAC [30]. Fig. 8 shows fairly homogeneous microporous size distributions. The pore volumes decreased with increasing amount of copper, as the copper particles blocked or were located on the pore walls. Detailed results on the textural properties of the samples are summarized in Table 1. The specific areas, average pore diameters, total and micropore volumes decreased with increasing deposition time. As summarized in Fig. 9, the steady-state NO

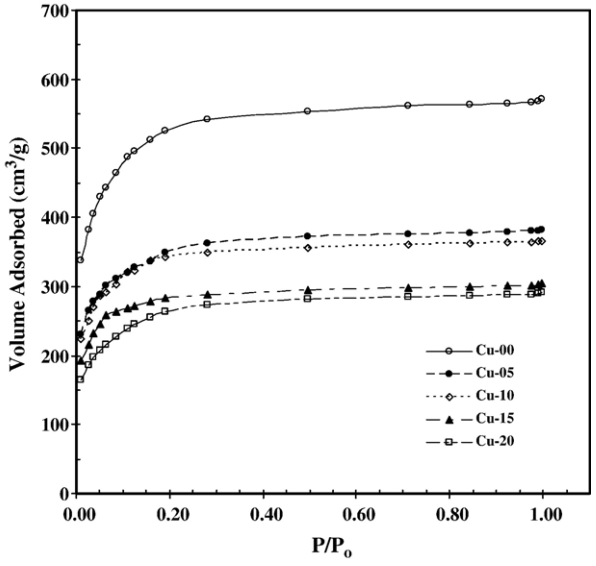

Fig. 7. Adsorption isotherms of N_2 at 77.4 K of pristine and copper-deposited ACF.

removal efficiency at all temperature was nearly zero (adsorption ≈ desorption) when pristine ACF were used. The NO removal efficiency was the highest when the amount was Cu/ACF = 110 mg/g (deposition time of 5 min), however, decreased at Cu/ACF beyond 110 mg/g (deposition times of 10, 15, 20 min) due to the decreased adsorption as a result of the increased amount of copper.

XRD and EDX analyses of copper-deposited ACF were carried out after they were used for NO removal tests. Part of copper particles was oxidized.

4. Conclusions

In the present study, pitch-based ACF were initially coated with copper fine particles using electroless copper deposition, and then characterized using FESEM, EDX, XRD, nitrogen adsorption and ICP analyses. The amount of copper particles was easily controlled by regulating the deposition time. Finally, the effect of copper particles on the catalytic reduction of NO was investigated at various reaction temperatures in the absence of oxygen.

Table 1
Textural properties of pristine and copper-deposited ACF

Sample	SSA[a] (m^2/g)	TPV[b] (cm^3/g)	MPV[c] (cm^3/g)	APD[d] (Å)
Cu-00	1590	0.87	0.77	11.6
Cu-05	1321	0.72	0.68	10.9
Cu-10	1201	0.66	0.61	10.6
Cu-15	1134	0.62	0.57	10.7
Cu-20	1029	0.56	0.53	10.5

[a]Specific surface area.
[b]Total pore volume.
[c]Micropore volume.
[d]Average pore diameter.

Pitch fibers were prepared from petroleum-derived IPPs using melt-blown spinning. After the fibers had been stabilized, carbonized, and thermally activated by steam, they (ACF) were then further activated with Pd–Sn catalytic nuclei in a single-step process. The catalytically activated ACF were used as supporters for the specific, electroless deposition of fine copper particles. The FESEM-EDX, ICP and XRD results show that the ACF were uniformly coated with nearly pure fine copper particles and that the amount of copper on the ACF increased with increasing deposition time.

With the copper particles-deposited onto the ACF, the NO removal efficiency was tested at four different deposition times (5, 10, 15 and 20 min). Experiments were performed in a packed bed tubular reactor under various reaction temperatures (423–673 K). For all deposition times, the NO removal efficiency increased with increasing reaction temperature up to 673 K. The

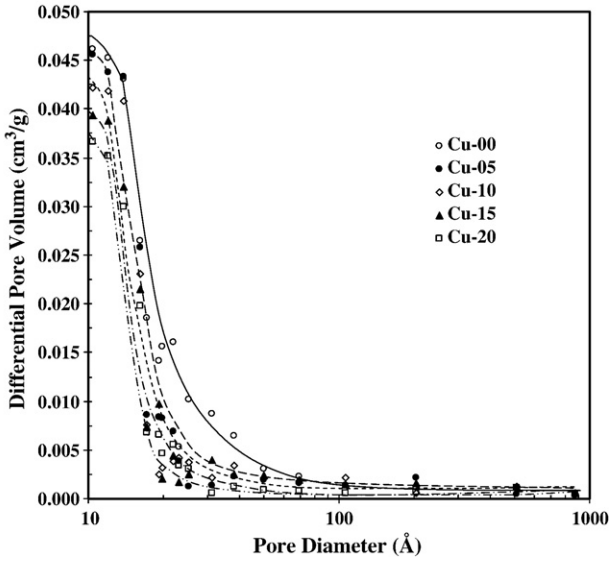

Fig. 8. Pore size distributions of pristine and copper-deposited ACF.

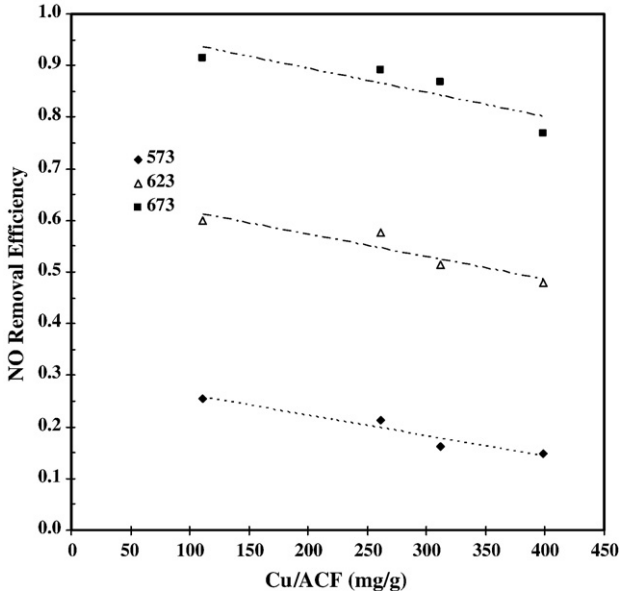

Fig. 9. Steady-state NO removal vs amount of copper.

NO removal efficiency was the highest when the amount was Cu/ACF = 110 mg/g (deposition time of 5 min), however, decreased at Cu/ACF beyond 110 mg/g (deposition times of 10, 15, 20 min) due to the decreased adsorption as a result of the increased amount of copper.

Acknowledgements

The authors acknowledge the support from the Korea Institute of Environmental Science and Technology project under grant 013-071-052. The authors also acknowledge the partial support from the Seoul Development Institute project (Grant no. 2006-8-1842).

References

[1] S.J. Park, B.J. Kim, J. Colloid Interface Sci. 282 (2005) 124.
[2] C.M. Yang, K. Kaneko, J. Colloid Interface Sci. 246 (2002) 34.
[3] J.S. Moon, K.K. Park, J.H. Kim, G. Seo, Appl. Catal., A Gen. 201 (2000) 81.
[4] S. Chen, H. Zeng, Carbon 41 (2003) 1265.
[5] Y. Matatov-Meytal, M. Sheintuch, Appl. Catal., A 231 (2002) 1.
[6] W. Shen, Q. Guo, Y. Zhang, Y. Liu, J. Zheng, J. Cheng, J. Fan, Colloids Surf., A 273 (2006) 147.
[7] P. Fu, Y. Luan, X. Dai, J. Mol. Catal., A 221 (2004) 81.
[8] S.H. Park, C. Kim, Y.I. Jeong, D.Y. Lim, Y.E. Lee, K.S. Yang, Synth. Met. 146 (2004) 207.
[9] C.Y. Li, Y.Z. Wan, J. Wang, Y.L. Wang, X.Q. Jiang, L.M. Han, Carbon 36 (1998) 61.
[10] I. Mochida, Y. Korai, M. Shirahama, S. Kawano, T. Hada, Y. Seo, M. Yoshikawa, A. Yasutake, Carbon 38 (2000) 227.
[11] E. Vilaplana-Ortego, J. Alcañiz-Monge, D. Cazorla-Amorós, A. Linares-Solano, Fuel Process. Technol. 77–78 (2002) 445.
[12] N. Shirahama, S.H. Moon, K.H. Choi, T. Enjoji, S. Kawano, Y. Korai, M. Tanoura, I. Mochida, Carbon 40 (2002) 2605.
[13] I. Mochida, S. Kawano, N. Shirahama, T. Enjoji, S.H. Moon, K.S. Sakanishi, Y. Korai, A. Yasutake, M. Yoshikawa, Fuel 80 (2001) 2227.
[14] Y.W. Lee, D.K. Choi, J.W. Park, Carbon 40 (2002) 1409.
[15] Z. Guo, Y. Xie, I. Hong, J. Kim, Energy Conv. Manag. 42 (2001) 2005.
[16] N. Shirahama, I. Mochida, Y. Korai, K.H. Choi, T. Enjoji, T. Shimohara, A. Yasutake, Appl. Catal., B 52 (2004) 173.
[17] J. Zawadzki, M. Wiśniewski, Carbon 40 (2002) 119.
[18] S. Adapa, V. Gaur, N. Verma, Chem. Eng. J. 116 (2006) 25.
[19] C. Marquez-Alvarez, I. Rodriguez-Ramos, A. Guerrero-Ruiz, Carbon 34 (1996) 339.
[20] M.J. Illán-Gómez, A. Linares-Solano, L.R. Radovic, C. Salinas-Martínez de Lecea, Energy Fuels 10 (1996) 158.
[21] S.J. Park, B.J. Kim, J. Colloid Interface Sci. 292 (2005) 493.
[22] W.H. Lin, C.Y. Hwang, H.F. Chang, Appl. Catal. A 162 (1997) 71.
[23] E. Norkus, A. Vaškelis, J. Jačiauskienė, I. Stalnionienė, G. Stalnionis, Electrochim. Acta 51 (2006) 3495.
[24] X. Zhao, K. Hirogaki, I. Tabata, S. Okubayashi, T. Hori, Surf. Coat. Technol. 201 (2006) 628.
[25] C. Fukuhara, Y. Kamata, A. Igarashi, Appl. Catal. A Gen. 296 (2005) 100.
[26] L.M. Ang, T.S. Andy Hor, G.Q. Xu, C.H. Tung, S. Zhao, J.L.S. Wang, Chem. Mat. 11 (1999) 2115.
[27] C. Xu, G. Wu, Z. Liu, D. Wu, T.T. Meek, Q. Han, Mater. Res. Bull. 39 (2004) 1499.
[28] J.H. Byeon, K.Y. Yoon, J.H. Park, J. Hwang, Carbon 45 (2007) 2313.
[29] M. Charbonnier, M. Romand, Y. Goepfert, D. Léonard, M. Bouadi, Surf. Coat. Technol. 200 (2006) 5478.
[30] S. Brunauer, P.H. Emmett, E. Teller, J. Am. Chem. Soc. 60 (1938) 309.